Korean J. Chem. Eng., 34(6), 1822-1826 (2017)
DOI: 10.1007/s11814-017-0068-3

pISSN: 0256-1115
eISSN: 1975-7220

Enhanced photoactivity of stable colloidal TiO_2 nanoparticles prepared in water by nanosecond infrared laser pulses

Yu Kwon Kim†, Gyuseong Lee, Yuna Kim, and Hyuk Kang†

Department of Chemistry and Department of Energy Systems Research, Ajou University, Suwon 16499, Korea
(*Received 13 December 2016 • accepted 7 March 2017*)

Abstract−A simple laser ablation technique was used to prepare a stable colloidal TiO_2 suspension in pure water. A transparent TiO_2 aqueous solution was obtained within a few minutes and its photoactivity for the degradation of methylene blue was measured to be higher than that of commercial TiO_2 nanoparticles. SEM analysis revealed that the average size of the nanoparticles increased from 20 to 40 nm as the laser power was raised from 0.5 to 2 W. The variation in size, however, had little influence on the resulting photodegradation rate under the given condition. Instead, the photodegradation rate is related to the number of colloidal TiO_2 particles in the aqueous solution, which increases proportionally to the ablation time. As the TiO_2 particle density increases, however, the photoactivity is measured to be gradually reduced due to the formation of TiO_2 aggregates. Thus, the optimum ablation time is 10-30 min under our ablation condition. Our results show that well-dispersed small TiO_2 nanoparticles of about a few tens nm can be readily formed by laser ablation within only a few minutes and can be used as highly efficient photocatalysts for photocatalytic remediation of water.

Keywords: Laser Ablation, TiO_2 Nanoparticles, Photocatalyst, Methylene Blue, Water Remediation

INTRODUCTION

Laser ablation has become a facile tool for synthesizing well-dispersed nanoparticles in liquid solution without any chemical precursors or ligands [1-3]. In addition, the particle size of various shaped nanoparticles can be adjusted in the range of a few nanometers [4,5]. Such advantages of laser ablation synthesis in liquid solution (LASiS) may be also applied to prepare colloidal oxide nanoparticles with high surface area [6,7], which may show high photocatalytic activity.

TiO_2 is not only chemically stable under ambient condition, but also shows a fascinating photocatalytic activity in photodegradation of organic dyes and photocatalytic water-splitting activity under UV illumination [8-10]. This makes TiO_2 a prototype oxide material for studying fundamental physicochemical processes associated with photocatalytic activity and the relation between photoactivity and physical properties such as size, bulk phase and morphology [11,12].

Laser ablation techniques have been frequently employed to prepare TiO_2 in various forms of nanostructured films [13,14], microtubes [15] and TiO_2 nanoparticles [16-19] for applications such as photocatalysts [6,19,20] and solar cells [21]. Here, detailed experimental conditions of laser ablation were found to be critical in determining various properties of the TiO_2 nanoparticles. Laser power and wavelength were reported to determine the final chemical composition and the detailed morphology of the TiO_2 nanostructures [22]. TiO_2 nanoparticles prepared in aqueous solution [16,17] could be obtained with high concentration of defects such as reduced Ti species (Ti^{x+}, x=2, 3), depending on the laser ablation conditions [16,18], which might provide a chance to observe enhanced photocatalytic activity of reduced blue (black) TiO_2 powders [17]. The controllability over size in the range of a few nm to a few tens nm of the technique may provide a chance of tuning the band gap in addition to its defect density in a favorable way to observe enhanced photoactivity. Ti-C bonds were introduced into amorphous TiO_x nanostructures by ablation of Ti in CO atmosphere in a vacuum chamber [14]. Bulk phase of TiO_2 was also shown to be selected between anatase and rutile by adjusting the focusing condition [18].

Motivated by such diverse studies on laser-ablated TiO_2, we performed a systematic investigation into the photocatalytic activity of laser-ablated TiO_2 nanoparticles. Photoactivity of laser ablated TiO_2 has been reported to be enhanced compared to commercial TiO_2 nanoparticles for photodegradation of methylene blue (MB) and antibacterial activity [19]. However, limited number of reports on the photoactivity of laser ablated TiO_2 nanoparticles are available and many details on the relation between the nature of laser-ablated TiO_2 and the resulting photoactivity are largely unknown. In this report, we present our systematic evaluation of photocatalytic activity of colloidal TiO_2 nanoparticles prepared in water by laser ablation at different laser power and ablation time. We found that a very stable colloidal suspension of TiO_2 nanoparticles in water can be prepared by properly selecting the laser power and ablation time. In addition, we show that the synthesized TiO_2 particles have a higher photoactivity compared to that of commercial ones measured under a similar condition.

†To whom correspondence should be addressed.
E-mail: hkang@ajou.ac.kr, yukwonkim@ajou.ac.kr

EXPERIMENTAL DETAILS

1. Laser-assisted Synthesis of TiO_2 Nanoparticles (L-TiO_2) in Aqueous Solution

A solid Ti sheet (1 cm×1 cm×1 mm, 99.5%, Nilaco) was placed at the center of a 50-mL beaker filled with 20 mL of deionized water maintained at room temperature (RT). Then, Nd:YAG laser (1,064 nm, 10 Hz, 10 ns, Spectra Physics, GCR 16-S) was focused onto the center of the Ti sheet using a lens with a focal length of 150 mm. The ablation time was varied in the range of 1-60 min at the laser power of 0.5-2 W. With 1 W and the average beam size of 0.25 mm^2, the power density was estimated to be ~400 W/cm^2 on the average but the peak power density was 4 GW/cm^2. After the laser irradiation, the resulting aqueous solution was still transparent to the naked eye without any visible precipitate for several days when the ablation time was lower than 30 min. Under typical ablation condition of 1.5 W at RT, the formation rate of TiO_2 in the aqueous solution was estimated to be about 10 μg/min from the weight loss of Ti. At a given focusing condition, the ablation rate increases with increasing laser power.

2. Characterization

The aqueous solution was sampled using a pipette, and a drop of the aqueous solution on a clean Si wafer was dried at room temperature. Aggregates of TiO_2 nanoparticles left on the Si wafer were investigated by a scanning electron microscope (FE-SEM, 5.0 kV, JSM 6700f, JEOL). SEM analysis was also performed to characterize the bulk phase of the TiO_2 nanoparticles formed by the laser ablation. Also, UV-Visible spectra of the aqueous solution were obtained using a UV-Vis spectrophotometer (S-3150, SCINCO).

3. Photoactivity Measurements

Photocatalytic activity of the TiO_2 nanoparticles was evaluated by measuring the initial photodegradation rate of methylene blue (MB) in aqueous solution under UV illumination (12 W, 365 nm). 14 mL of the aqueous solution with TiO_2 nanoparticles was mixed with concentrated MB solution to obtain 100 mL of solution with the initial MB concentration of 0.01 mM. TiO_2 concentration increased up to 60 mg/L with increasing ablation time to 1 h. The absorbance of MB at 665 nm was monitored using a UV-Vis spectrophotometer at room temperature. Initial reaction rate constant (min^{-1}) was obtained from the slope in the plot of natural log of MB concentration vs. time by assuming that the first-order reaction kinetics. The measured photoactivity was compared with that of our reference solution with a commercial TiO_2 (p-25, 60 mg/L) under the same MB concentration.

RESULTS AND DISCUSSION

TiO_2 nanoparticles prepared in deionized water by pulses of a focused laser are not visible by the naked eye since the aqueous solution remains to be transparent (up to the ablation time of about 30 min) until white precipitates are formed upon prolonged laser irradiation (e.g., above 40 min). Instead, the formation of nanometer-sized TiO_2 particles is confirmed from the SEM images shown in Fig. 1. For the SEM measurement, a few (2-3) drops of the aqueous solution on a clean Si(100) wafer were vaporized to obtain precipitated aggregates of nanoparticles on the Si substrate. The SEM

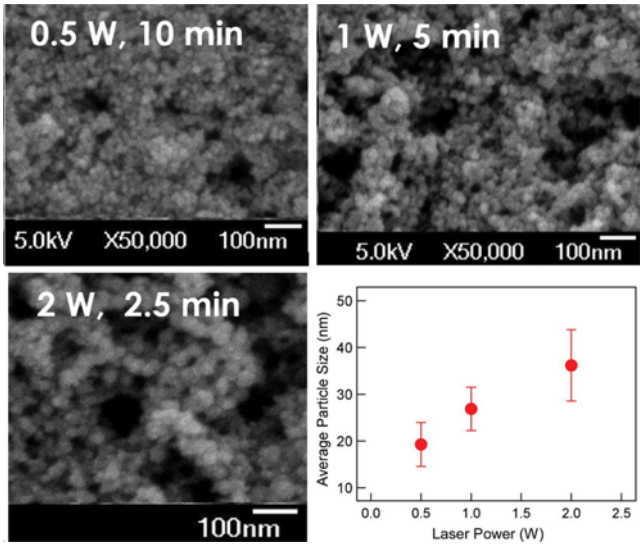

Fig. 1. SEM images of TiO_2 nanoparticles prepared by laser ablation at various laser powers of 0.5-2 W. Also, shown in the graph is the plot of the size of the particles vs. the laser power used.

images of the precipitates show spherically shaped nanoparticles of marginally uniform size. Also, the particle size increases as the laser power increases from 0.5 W to 2 W. The size of TiO_2 nanoparticles remains to be about the same at the given laser power, especially in the initial stage of ablation (e.g., up to 10 min) at which the TiO_2 concentration can be assumed to be low. Thus, the laser power is the factor in determining the size of TiO_2 nanoparticles in the solution. At longer ablation times, the agglomeration of TiO_2 particles makes it hard to determine the size of TiO_2 nanoparticles. The particle size distribution determined from the SEM images of Fig. 1 is plotted against the laser power in the same figure. We find that the average diameter of the particles increases from ~20 nm at 0.5 W to ~40 nm at 2 W.

Earlier studies show that the size of nanoparticles depends on a number of laser parameters as well as the kind of chemical species (e.g., surfactants) in the solution. In our case, the solution was a pure deionized water without any surfactant. Thus, the observed particle size can be assumed to be a result of the vaporization of Ti metal via melting in aqueous solution by absorption of the focused nanosecond laser [23,24]. The hot Ti vapor reacts with H_2O to form oxide particles as it diffuses away from the laser spot. Higher laser power under the same experimental conditions (e.g., the size of the focus and pulse width, etc.) would induce higher temperature of the focused spot on Ti metal, which can produce Ti vapors with higher density under a single shot of laser pulse. Larger size of oxide nanoparticles is expected when the precursor density is higher.

The effect of post irradiation on the size of nanoparticles is negligible in our case. Particles may undergo fragmentation in the liquid phase via post irradiation, especially for shorter pulse durations [25]. In our experimental condition, however, the laser beam is focused onto the metal surface and the TiO_2 nanoparticles in the liquid phase do not absorb light at 1,064 nm due to the large bandgap (>3.0 eV) of TiO_2. Thus, the post-heating effect of the nanoparticles can be safely assumed to be negligible.

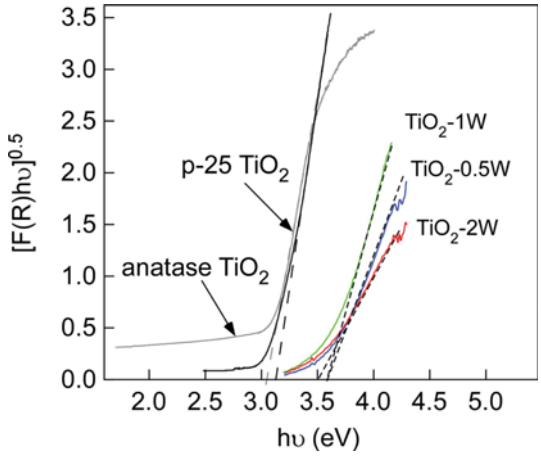

Fig. 2. A Kubelka-Munk plot of UV-vis spectra of the aqueous colloidal TiO_2 solutions prepared at the laser powers of 0.5, 1 and 2 W for the ablation time of 30 min.

The transparent colloidal TiO_2 nanoparticles in aqueous solution were further analyzed from UV-vis spectra by plotting $[F(R)hv]^{0.5}$ vs. hv where F(R) is Kubelka-Munk function in Fig. 2. From this analysis, the bandgap of our TiO_2 nanoparticles prepared by laser ablation was measured in the range of 3.5-3.6 eV. Also, shown in the graph is the spectrum of our anatase TiO_2 nanocrystals prepared by a typical hydrothermal method [26]. Typical anatase TiO_2 nanocrystals of ~100 nm in size prepared by a hydrothermal method and most commercial TiO_2 particles (e.g., p-25) usually have an indirect bandgap of 3.0-3.2 eV. Thus, the bandgap of our TiO_2 nanoparticles (~3.5 eV) is somewhat higher than the typical value of larger TiO_2 particles.

Particle size is an important parameter in various physical and chemical properties of semiconductor nanoparticles [27,28]. Smaller particles may have larger bandgap, which shifts the absorption band edge to higher wavelength due to quantum size effect [27,29,30], as in the case of CdS and ZnS, for example; a larger bandgap is obtained from the smaller nanoparticles. In our case, the bandgap of 3.5-3.6 eV for our TiO_2 nanoparticles was definitely higher than the typical value of TiO_2 particles (3.0-3.2 eV). Also, slightly higher bandgap of 3.6 eV for smaller (20-30 nm) TiO_2 (TiO_2-0.5W and TiO_2-1W) was observed than that (3.5 eV) of larger (~40 nm) TiO_2 (TiO_2-2W).

The band gap of small TiO_2 nanoparticles was measured in a wide range of 2.9-3.6 eV, depending on the detailed preparation conditions. Studies on anatase TiO_2 particles with size in the range of 1-50 nm indicate that the bandgap was blue-shifted by about 0.1-0.2 eV from 3.2 eV as the particle size decreased [29-32]. Even higher blue-shift of 0.4-0.6 eV for smaller TiO_2 particles (<5 nm) has been also reported [33]. In other cases, the bandgap has been observed not to strictly follow the size of TiO_2 particles in the range of 2-30 nm and has been attributed to direct transitions in indirect bandgap TiO_2 nanocrystals [34]. In fact, the bandgap of TiO_2 nanoparticles is not only influenced by the size of the particles, but also by the effective mass of the excitons [35,36], which can vary significantly depending on the bulk phase, shape and any change in lattice constant induced by a strain in small clusters. Possibly

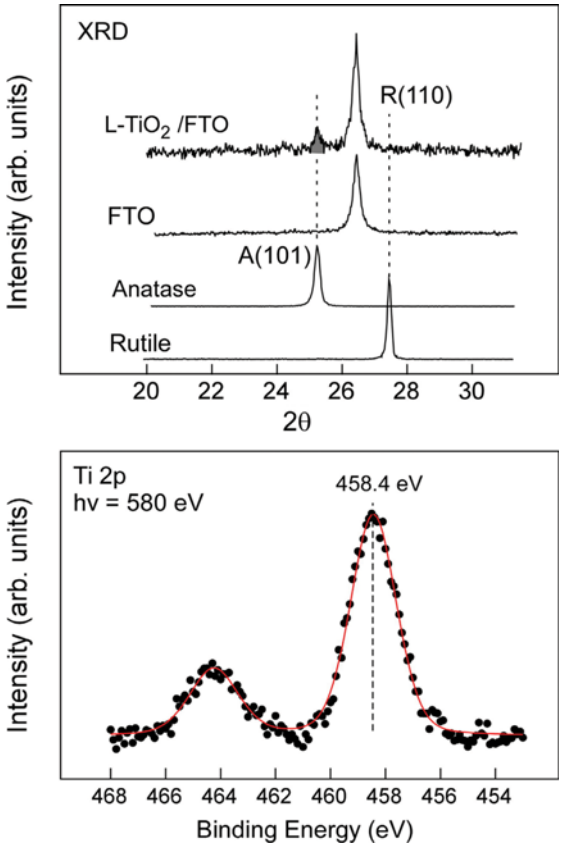

Fig. 3. (a) XRD spectrum of TiO_2-1W deposited on FTO is compared with those of the substrate (FTO), standard anatase TiO_2 and rutile TiO_2 powders obtained in our lab. (b) Ti 2p core level spectrum of TiO_2-1W deposited on a clean Si(100) wafer taken with hv=580 eV.

the reduced effective mass of excitons in small TiO_2 nanoparticles may induce a blue-shift in the measured absorption edge, which may be the case of ours.

The bulk phase of our L-TiO_2 was evaluated by taking XRD spectrum as shown in Fig. 3(a). Since the TiO_2 suspension is coated on FTO substrate, the XRD pattern shows an intense peak originates from the substrate. In addition, we can see a small peak at 2θ= 25.2, which is assigned to the (101) peak of anatase TiO_2 [37]. No rutile phase is detected in our case. From the Ti 2p core level spectrum of TiO_2-1W shown in Fig. 3(b), the Ti $2p_{3/2}$ peak at 458.4 eV is attributed to the Ti^{4+} of stoichiometric TiO_2 [38,39]. Thus, we conclude that the focused nanosecond laser pulse of 1,064 nm onto Ti metal in water at RT produces anatase TiO_2 nanoparticles of a few tens nm in size well dispersed as a colloid in aqueous phase without any further post-treatments, which is also quite stable for several days.

In Fig. 4, we evaluated photoactivity of our TiO_2 suspension in water by measuring initial rate constant of the photodegradation reaction of MB under UV light as described in the experimental section. The wavelength (365 nm) of the UV light employed corresponds to 3.4 eV, which is close to the nominal bandgap determined from Fig. 2. Still, we observed a reasonably good photoactivity that is comparable to that of a commercial TiO_2 powder (P-25). Here,

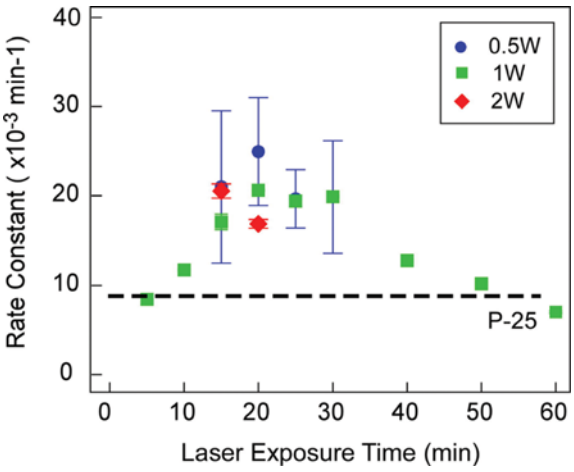

Fig. 4. Photodegradation rates of methylene blue over our TiO_2 nanoparticles prepared by laser ablation at the laser power of 0.5-2 W. The initial rate constants are plotted against the ablation time at each laser power.

the photoactivity measurement condition is very similar between the two cases (laser-ablated TiO_2 and P-25), except that the laser-ablated TiO_2 concentration is estimated to be much lower than that of P-25 (0.06 g/L); considering the ablation rate, about 60 min corresponds to the same concentration of TiO_2 as that (0.06 g/L) of P-25. Thus, at 5 min, the TiO_2 concentration is estimated to be about one order-of-magnitude lower than that of P-25. Despite the low concentration of TiO_2, we observed that the photodegradation rates of our laser-ablated TiO_2 (0.5-2 W) are generally higher than that of P-25 when the ablation time is above 5 min. At lower ablation time (<5 min), the low photoactivity can be attributed to low concentration of TiO_2 particles in the water. At higher ablation time (>40 min), the photoactivity also decreases regardless of the laser power employed (0.5-2 W). It is an interesting observation since the TiO_2 concentration is expected to increase further (even though it is not linear) in proportion to the ablation time.

We speculate that the formation of white visible TiO_2 aggregates may result in a decrease in the effective surface area of TiO_2 particles for photoreaction in the solution. The white TiO_2 aggregates start to form when the ablation time increases above 20-30 min. At higher laser power (2 W), the aggregate formation starts early (~20 min), while it can be delayed to ~30 min or longer at lower laser power (0.5 W). This fact suggests that the TiO_2 aggregates are formed when the TiO_2 particle density increases above a certain critical value in the water; when the laser power is higher, the critical density is achieved at a shorter ablation time. When the aggregates are formed, the overall surface area exposed to the reactant molecules for photodegradation may decrease. Also, the murky water with the aggregates may reduce the UV transmission deep in the bottom of the solution. Combined together, this is attributed to the reason for the decrease in photoactivity in this region. Thus, the shape of the graph in Fig. 4 follows a volcano-like shape; the increase in photoactivity with increasing density of TiO_2 is compensated by the decrease due to the formation of aggregates.

Although we found a strong relation between photoactivity and the ablation time, the laser power is shown to have a little effect on the photoactivity. The photoactivity measurements are in general influenced by number of factors, such as a slight change in pH, unknown TiO_2 concentration and possibly the presence of unknown impurities, which are the origin of the high uncertainty in the measured rate constants. Thus, the data shown are the average value with error bars of at least 5-10 measurements. Although only a few measurements were performed for the cases of 0.5 and 2 W, the measured activity falls into the data set for 1 W, suggesting that the laser power (or power-dependent variation in size) is weakly correlated to the overall photoactivity. The increased ablation rate with increasing laser power may be compensated by the increased particle size, which results in a little change in the density of TiO_2 particles. This in turn implies that the particle size of TiO_2 in the range of 10-40 nm has little influence on the photoactivity. Any further investigation into the relation between the physical properties of TiO_2 particles and photoactivity with higher precision will be a subject for our future study.

The measured high activity of laser-ablated TiO_2 compared to that of P-25 (0.06 g/L) suggests that laser ablation is a simple and efficient technique for producing small TiO_2 particles with high surface area, which shows enhanced photoactivity at low concentration (~mg/L); the TiO_2 concentration is estimated to increase up to about 6 mg/L at the ablation time of 60 min. Considering the enhanced activity of the laser-ablated TiO_2, this technique can be applied to the production of TiO_2-based photocatalysts in water for environmental remediation. Also, it can be extended to producing doped TiO_2 particles with a narrow bandgap for a visible response by simply adding other chemical ingredients or surfactants in water too. The TiO_2 particles may be deposited on a porous matrix in a form of mesh as a support for the reuse of the catalysts in a flowing reactor. Combined with the fact that inexpensive laser sources are available these days, such a diverse variation of the technique makes laser ablation promising in the future development of environment-friendly oxide photocatalysts.

CONCLUSIONS

A stable colloidal suspension of TiO_2 nanoparticles was prepared in water by a simple laser ablation technique at RT. The nanoparticles produced were found to be a stoichiometric TiO_2 in anatase phase and of a few tens of nanometers in size. The laser power and the ablation time were found to control the size and the density of TiO_2 nanoparticles, respectively. The size of the TiO_2 nanoparticles increased with increasing laser power and the density of the TiO_2 particles in the aqueous solution increased with the ablation time. The resulting solution was found to exhibit higher activity in photodegradation of MB under UV irradiation than P-25 at lower TiO_2 concentration. The ablation time for the high activity was 10-30 min at the laser power of 0.5-2 W with the nanosecond infrared laser employed in this study. As the particle density increases, the colloidal stability is lifted to induce the formation of TiO_2 aggregates, resulting in a decrease in photoactivity due to the reduced surface area. Thus, we can conclude that the high photoactivity of the laser-ablated TiO_2 solution at the low concentration is due to the high surface area associated with the stable colloidal suspension of the small TiO_2 nanoparticles.

ACKNOWLEDGEMENT

This research was supported by Basic Science Research Program (2012R1A1A2007641 and 2013R1A1A2008708) through the National Research Foundation of Korea (NRF) funded by the Ministry of Education, Science and Technology. This work was also supported by an Ajou University research fund.

COMPLIANCE WITH ETHICAL STANDARDS

Conflict of interest The authors declare that they have no conflict of interest.

REFERENCES

1. R. Intartaglia, G. Das, K. Bagga, A. Gopalakrishnan, A. Genovese, M. Povia, E. Di Fabrizio, R. Cingolani, A. Diaspro and F. Brandi, *Phys. Chem. Chem. Phys.*, **15**, 3075 (2013).
2. S. Barcikowski and G. Compagnini, *Phys. Chem. Chem. Phys.*, **15**, 3022 (2013).
3. T. E. Itina, *J. Phys. Chem. C*, **115**, 5044 (2011).
4. B. C. Lin, P. Shen and S. Y. Chen, *J. Phys. Chem. C*, **115**, 5003 (2011).
5. R. Intartaglia, K. Bagga, F. Brandi, G. Das, A. Genovese, E. Di Fabrizio and A. Diaspro, *J. Phys. Chem. C*, **115**, 5102 (2011).
6. M. Ikeda, Y. Kusumoto, H. Yang, S. Somekawa, H. Uenjyo, M. Abdulla-Al-Mamun and Y. Horie, *Catal. Commun.*, **9**, 1329 (2008).
7. H. Wang, N. Koshizaki, L. Li, L. Jia, K. Kawaguchi, X. Li, A. Pyatenko, Z. Swiatkowska-Warkocka, Y. Bando and D. Golberg, *Adv. Mater.*, **23**, 1865 (2011).
8. K. Hashimoto, H. Irie and A. Fujishima, *Jpn. J. Appl. Phys.*, **44**, 8269 (2005).
9. M. Ni, M. K. H. Leung, D. Y. C. Leung and K. Sumathy, *Renewable Sustainable Energy Rev.*, **11**, 401 (2007).
10. C. Y. Teh, T. Y. Wu and J. C. Juan, *Chem. Eng. J.*, In Press (2017), DOI:10.1016/j.cej.2017.01.001.
11. A. L. Linsebigler, G. Lu and J. T. Yates, *Chem. Rev.*, **95**, 735 (1995).
12. S. G. Kumar and L. G. Devi, *J. Phys. Chem. A*, **115**, 13211 (2011).
13. E. C. Landis, K. C. Phillips, E. Mazur and C. M. Friend, *J. Appl. Phys.*, **112**, 063108 (2012).
14. V. Jandová, J. Kupčík, Z. Bastl, J. Šubrt and J. Pola, *Solid State Sci.*, **19**, 104 (2013).
15. A. De Bonis, A. Galasso, N. Ibris, A. Laurita, A. Santagata and R. Teghil, *Appl. Surf. Sci.*, **268**, 571 (2013).
16. C.-N. Huang, J.-S. Bow, Y. Zheng, S.-Y. Chen, N. Ho and P. Shen, *Nanoscale Res. Lett.*, **5**, 972 (2010).
17. E.-C. Chang, B.-C. Lin, P. Shen and S.-Y. Chen, *J. Nanosci. Nanotechnol.*, **12**, 8337 (2012).
18. A. Nath, S. S. Laha and A. Khare, *Appl. Surf. Sci.*, **257**, 3118 (2011).
19. M. Zimbone, M. A. Buccheri, G. Cacciato, R. Sanz, G. Rappazzo, S. Boninelli, R. Reitano, L. Romano, V. Privitera and M. G. Grimaldi, *Appl. Catal., B*, **165**, 487 (2015).
20. G. Panomsuwan, A. Watthanaphanit, T. Ishizaki and N. Saito, *Phys. Chem. Chem. Phys.*, **17**, 13794 (2015).
21. V. Korstgens, S. Proller, T. Buchmann, D. Mosegui Gonzalez, L. Song, Y. Yao, W. Wang, J. Werhahn, G. Santoro, S. V. Roth, H. Iglev, R. Kienberger and P. Muller-Buschbaum, *Nanoscale*, **7**, 2900 (2015).
22. N. Ohtsu, K. Kodama, K. Kitagawa and K. Wagatsuma, *Appl. Surf. Sci.*, **256**, 4522 (2010).
23. S. Nolte, C. Momma, H. Jacobs, A. Tünnermann, B. N. Chichkov, B. Wellegehausen and H. Welling, *J. Opt. Soc. Am. B*, **14**, 2716 (1997).
24. R. Kelly and A. Miotello, *Appl. Surf. Sci.*, **96-98**, 205 (1996).
25. S. Besner, A. V. Kabashin and M. Meunier, *Appl. Phys. Lett.*, **89**, 233122 (2006).
26. X. Yu, B. Kim and Y. K. Kim, *ACS Catal.*, **3**, 2479 (2013).
27. Y. Wang and N. Herron, *J. Phys. Chem.*, **95**, 525 (1991).
28. C. N. R. Rao, G. U. Kulkarni, P. J. Thomas and P. P. Edwards, *Chem. Eur. J.*, **8**, 28 (2002).
29. L. Kavan, T. Stoto, M. Graetzel, D. Fitzmaurice and V. Shklover, *J. Phys. Chem.*, **97**, 9493 (1993).
30. W. Choi, A. Termin and M. R. Hoffmann, *J. Phys. Chem.*, **98**, 13669 (1994).
31. M. Anpo, T. Shima, S. Kodama and Y. Kubokawa, *J. Phys. Chem.*, **91**, 4305 (1987).
32. C. Kormann, D. W. Bahnemann and M. R. Hoffmann, *J. Phys. Chem.*, **92**, 5196 (1988).
33. E. Joselevich and I. Willner, *J. Phys. Chem.*, **98**, 7628 (1994).
34. N. Serpone, D. Lawless and R. Khairutdinov, *J. Phys. Chem.*, **99**, 16646 (1995).
35. L. Brus, *J. Phys. Chem.*, **90**, 2555 (1986).
36. J. J. Kasinski, L. A. Gomez-Jahn, K. J. Faran, S. M. Gracewski and R. J. D. Miller, *J. Chem. Phys.*, **90**, 1253 (1989).
37. D. Reyes-Coronado, G. Rodríguez-Gattorno, M. E. Espinosa-Pesqueira, C. Cab, R. de Coss and G. Oskam, *Nanotechnology*, **19**, 145605 (2008).
38. C. Y. Teh, T. Y. Wu and J. C. Juan, *Catal. Today*, **256**, 365 (2015).
39. A. Calloni, A. Brambilla, G. Berti, G. Bussetti, E. V. Canesi, M. Binda, A. Petrozza, M. Finazzi, F. Ciccacci and L. Duò, *Langmuir*, **29**, 8302 (2013).